Model of Noncritical Concentration Fluctuations in Binary Liquids. Verification by Ultrasonic Spectrometry of Aqueous Systems and Evidence of Hydrophobic Effects

A. Rupprecht and U. Kaatze*

Drittes Physikalisches Institut, Georg-August-Universität, Bürgerstrasse 42-44, D-37073 Göttingen, Germany

Received: March 12, 1999

This work is based on the experimental evidence from ultrasonic absorption spectra, measured between about 100 kHz and 5 GHz for some series of liquid mixtures with water as a constituent. Since none of the existing models of noncritical concentration fluctuations appropriately applies for the shape of the existing set of spectra, a comprehensive theoretical model has been derived which includes the favorable characteristics of previous theories. In this model, fluctuations in concentration are assumed to equalize not only by diffusion but, in parallel, also by a specific rate process. In addition, allowance is made for spatial correlations in the concentration fluctuations. Discussion of the measured ultrasonic spectra in terms of the comprehensive model evidences the effect from the hydrophobic properties of the nonaqueous constituent of the mixtures upon the microheterogeneous structure of the liquid.

1. Introduction

During the past years much attention has been directed toward the microinhomogeneous structure of binary liquids. Interest in the liquid microheterogeneity and its accompanying fluctuations of thermodynamic parameters does not just spring from its import for our fundamental understanding of liquids, including aspects of universality and dynamic scaling. It also results from a variety of applications in biophysics, physical chemistry, and in chemical engineering as well.

The dynamic properties of critical binary systems of nonassociating constituents are well established now. Nevertheless, there appear to exist three important areas in which our present knowledge of the microheterogeneity of liquids is still rather poor. (i) Theoretical treatments of the dynamic behavior of critical systems is restricted to the close vicinity of a critical point. Only recently the cross-over region between critical and noncritical systems has been considered both theoretically and experimentally.[1,2] (ii) Ultrasonic attenuation spectra of critical mixtures of associating liquids always show contributions with relaxation characteristics, in excess of the contribution predicted by existing theories of concentration fluctuations.[3,4] (iii) Rather unexpectedly, a multitude of binary aqueous systems exhibit a microinhomogeneous structure and display features of noncritical concentration fluctuations. Among these systems are mixtures of water with monohydric alcohols,[5] poly(ethylene glycol)-monoalkyl ethers C_iE_j,[6] tetraalkylammonium bromides,[7] triethylenediamine,[8] and derivatives of urea.[9] Again, however, the existing theoretical models do not satisfactory apply for all measured spectra. Therefore, even theories that had been originally designed for the description of critical systems[10−13] have been empirically used to represent experimental findings for noncritical mixtures.[5]

For a noncritical aqueous solution of the alkyl polyglycol ether C_4E_2, the discrepancy between theoretical predictions and measured spectra is illustrated by an example given in Figure 1. In that diagram the excess attenuation per wavelength $(\alpha\lambda)_{exc}$, is displayed as a function of frequency ν. Here

$$(\alpha\lambda)_{exc} = \alpha\lambda - B\nu \qquad (1)$$

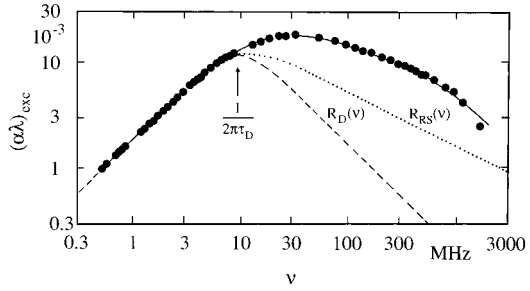

Figure 1. Ultrasonic excess attenuation per wavelength, $(\alpha\lambda)_{exc}$, at 25 °C displayed as a function of frequency ν for a mixture of water and 2-(2-butoxyethoxy)ethanol (C_4E_2) with mole fraction $x = 0.04$ of C_4E_2. The dotted and dashed curves are graphs of a Romanov−Solov'ev term (eq 3) and a Debye relaxation spectral term (eq 2), respectively. The full curve represents the spectral term of the unifying model (eq 22).

is the part of the total attenuation per wavelength $\alpha\lambda$ that exceeds the high-frequency asymptotic part $B\nu$. In eq 1 α is the attenuation coefficient, $\lambda = c_s/\nu$ is the wavelength, c_s is the sound velocity, and B denotes a frequency independent coefficient. Also presented in Figure 1, for comparison with the excess attenuation spectrum, is the graph of a Debye type relaxation spectral term[14] ($\omega = 2\pi\nu$)

$$R_D(\nu) = A_D \frac{\omega\tau_D}{1 + (\omega\tau_D)^2} \qquad (2)$$

with discrete relaxation time τ_D and with relaxation amplitude A_D. Obviously, a Debye term cannot account for the measured data. This is particularly true at high frequencies ($\omega \gg \tau_D^{-1}$) where eq 2 predicts an ω^{-1} behavior, at variance with the experimental data. In conformity with the assumption of a diffusive process, these data in part of the frequency range decrease rather proportionally to $\omega^{-1/2}$, thus indicating that the cause of the sonic relaxation is not a stoichiometrically well defined chemical equilibrium but rather a concentration fluctuation mechanism. For this reason, additionally given in Figure 1 is the graph of the term

10.1021/jp9908810 CCC: $18.00
Published on Web 07/28/1999

$$R_{RS}(\nu) = A_{RS}\omega\tau_{RS}I_{RS}(\omega\tau_{RS}) \quad (3)$$

which is based on the prominent theory of noncritical concentration fluctuations, the Romanov−Solov'ev model.[15−18] Written in the format of eq 3, A_{RS} is a frequency-independent amplitude and I_{RS} is a scaling function. The integral I_{RS} can be given in an explicit form:

$$I_{RS}(\omega\tau_{RS}) = 3 - \frac{3\sqrt{\omega\tau_{RS}}}{4\sqrt{2}}\left[2\pi - ln\frac{\omega\tau_{RS} - \sqrt{2\omega\tau_{RS}} + 1}{\omega\tau_{RS} + \sqrt{2\omega\tau_{RS}} + 1} - 2\arctan(\sqrt{2\omega\tau_{RS}} + 1) - 2\arctan(\sqrt{2\omega\tau_{RS}} - 1)\right] \quad (4)$$

The relaxation time

$$\tau_{RS} = l_m^2/D \quad (5)$$

is a diffusion time, D is the mutual diffusion coefficient, and l_m is a minimum interaction length of fluctuations. This empirical parameter l_m has been introduced in the theory just to allow for the explicite form of the scaling function.

The spectrum for the C_4E_2/water mixture shown in Figure 1 also is only incompletely represented by the Romanov−Solov'ev term $R_{RS}(\nu)$. In particular, the width of the $R_{RS}(\nu)$ term is insufficient to adequately account for the measured data, extending over a broader frequency band. It has been shown recently[7] that the width of the R_{RS} term increases if spatial correlations of concentration fluctuations are taken into account, which in the original Romanov−Solov'ev theory are assumed to be absent. Even the consideration of such correlations, however, does not result in a spectral term that allows for a satisfactory description of all existing ultrasonic attenuation spectra under consideration. This situation, and also the need for the somewhat artificial l_m parameter in the original Romanov−Solov'ev theory, has prompted us to rederive a theoretical model of concentration fluctuations and of their effects in the ultrasonic attenuation spectra of binary liquids. Here we present a comprehensive treatment, taking into account the merits of the previous theories.[7,15−20] It turned out that this model allows for a uniform description of all broadband ultrasonic spectra under investigation.[5−9] Applying the comprehensive model, we also found unexpected correlations between the tendency of an aqueous system to form a microinhomogeneous structure and the hydrophobic properties of the second constituent of the mixture. These correlations are also briefly discussed in this article.

2. Concentration Fluctuation Model

Let $\rho(\vec{r}, t)$ denote an order parameter which represents the fluctuation amplitude of the local structure at time t around the point $\vec{r}$. For the binary liquids under consideration a most suitable order parameter is the deviation of the local molar concentration $c(\vec{r},t)$ from the mean $\bar{c}$. Hence

$$\rho(\vec{r},t) = c(\vec{r},t) - \bar{c} \quad (6)$$

The time dependence of local fluctuations may then be expressed by the autocorrelation function of the order parameter

$$\phi(\vec{r},t) = \langle\rho(\vec{r},t)\rho(\vec{0},0)\rangle/\langle|\rho(\vec{0},0)|^2\rangle \quad (7)$$

Changes in the local structure of the liquids are assumed to be enabled along two different pathways, following either an elementary chemical reaction with discrete relaxation time τ_0 or a diffusive process with diffusion coefficient D of the order parameter. The chemical process, associated with an activation barrier $\Delta H^{\ddagger}$, with a reaction volume, ΔV, and/or with a reaction enthalpy ΔH, may consist in a jump of a molecule from a position $\vec{r}_1$ to another one $\vec{r}_2$. Frequently it will be related to a dimerization reaction as assumed by Endo.[20] Because to these presumptions, the time behavior of the fluctuations is controlled by the differential equation

$$\partial\phi(\vec{r},t)/\partial t = (D\nabla^2 - 1/\tau_0)\phi(\vec{r},t) \quad (8)$$

Spatial Fourier transformation yields

$$\hat{\phi}(\vec{q},t) = \int_{\vec{r}}\phi(\vec{r},t)\exp(i\vec{r}\,\vec{q})\mathrm{d}\vec{r} \quad (9)$$

with the wave vector $\vec{q}$. The simpler differential equation

$$\partial\hat{\phi}(\vec{q},t)/\partial t = -(1/\tau_g)\hat{\phi}(\vec{q},t) \quad (10)$$

follows for the q space. Here

$$\tau_g^{-1} := \tau_q^{-1} + \tau_0^{-1} = Dq^2 + \tau_0^{-1} \quad (11)$$

where $q = |\vec{q}|$. In isotropic liquids the correlations in fluctuations will depend on $r = |\vec{r}|$ only. Equation 10 is solved by exponentials with characteristic decay time τ_g for each Fourier component

$$\hat{\phi}(q,t) = \hat{f}(q)\exp(-t/\tau_g) \quad (12)$$

The weight function $\hat{f}(q)$ is the Fourier transform of the spatial correlations $\phi(r,0)$ in the fluctuations at time $t = 0$. Hence suitable initial conditions $\phi(r,0)$ allow $\hat{f}(q)$, and thus the desired $\hat{\phi}(q,t)$, to be calculated. Romanov and Solov'ev[15,16] in their model neglected spatial correlations of fluctuations and took

$$\phi_{RS}(r,0) \propto \delta(r) \leftrightarrow \hat{f}_{RS}(q) = \text{constant} \quad (13)$$

Montrose and Litovitz[19] proposed an exponential decay with characteristic length ξ

$$\phi_{ML}(r,0) \propto \exp(-r/\xi) \leftrightarrow \hat{f}_{ML}(q) \propto (1 + (q\xi)^2)^{-2} \quad (14)$$

Endo[20] and Kühnel et al.[7] preferred an Ornstein−Zernike ansatz[21,22]

$$\phi_E(r,0) \propto (1/r)\exp(-r/\xi) \leftrightarrow \hat{f}_E(q) \propto (1 + (q\xi)^2)^{-1} \quad (15)$$

Here we propose the weight function

$$\hat{f}(q) \propto (1 + 0.164(q\xi) + 0.25(q\xi)^2)^{-2} \quad (16)$$

Using this function the long range correlations in fluctuations are assumed to follow the Ornstein−Zernike behavior. This means that, at long distances ($r \geq \xi$), where direct interactions between two "particles" can be neglected, correlations are mediated indirectly by interactions with neighboring "particles".[28] This assumption has been proven useful in a recent description of concentration fluctuations in aqueous solutions of tetraalkylammonium bromides,[7] where long ranging Coulombic forces act their influence on the spatial distribution of "particles". In close similarity to the Montrose−Litovitz model,[19] short range correlations are considered in eq 16 by a nearly exponential decay at $r < \xi$. In Figure 2 the $\hat{f}(q)$ function (eq 16) is compared to the corresponding weight functions $\hat{f}_{ML}(q)$

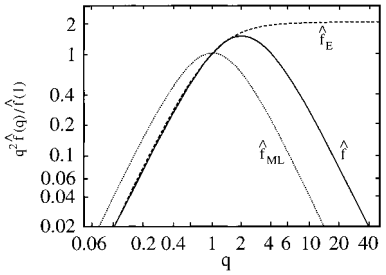

Figure 2. Relative weights of the spectral contributions at wave number q displayed for the present model ($\hat{f}$, full curve, eq 16) as well as for the Montrose−Litovitz ($\hat{f}_{ML}$, dotted curve) and Endo ($\hat{f}_E$, dashed curve) model.

and $\hat{f}_E(q)$ of the Montrose−Litovitz and Endo models, respectively. As will become evident below, by the particular choice of the coefficients in the $\hat{f}(q)$ function the present model combines an Ornstein−Zernike behavior of long range interactions with the integrability of the scaling function, without the need for the introduction of a somewhat artificial minimum interaction length l_m (eq 5).

Assuming a Debye density of states, $Vq^2/(2\pi^2)$, for the distribution of wave numbers q on the surface of a sphere of volume V, the spectral density $\langle|\delta\tilde{X}(\omega)|^2\rangle$ of fluctuations $\delta X(\vec{r},t)$ of a thermodynamic quantity X can be calculated according to linear system theory

$$\langle|\delta\tilde{X}(\omega)|^2\rangle \propto \frac{V}{2\pi^2}\int_0^\infty q^2 Re(\tilde{\phi}(q,\omega))\,\mathrm{d}q \tag{17}$$

Here $\tilde{\phi}(q,\omega)$ is the Fourier transform of $\hat{\phi}(q,t)$. Hence

$$Re(\tilde{\phi}(q,\omega) = \frac{1}{2\pi}\hat{f}(q)\frac{\tau_g}{1+\omega^2\tau_g^2} \tag{18}$$

and

$$\langle|\delta\tilde{X}(\omega)|^2\rangle \propto \frac{V}{4\pi^3}\int_0^\infty q^2\hat{f}(q)\frac{\tau_g}{1+\omega^2\tau_g^2}\mathrm{d}q \tag{19}$$

The integral on the right hand side of this relation exists only if toward high wavenumbers $\hat{f}(q)$ decreases more rapidly than q^{-2}. For this reason, in previous theories[7,15−18,20] integration has been performed over the interval from 0 to a maximum value q_{max}. This value has then been interpreted as to be due to a minimum interaction length $l_m = 2\pi q_{max}^{-1}$, as mentioned afore.

Consider $\delta\tilde{X}(\omega)$ the response of a linear system to a harmonically oscillating driving force $\delta\tilde{Y}(\omega)$ so that

$$\delta\tilde{X}(\omega) = \chi(\omega)\delta\tilde{Y}(\omega) \tag{20}$$

with the complex susceptibility $\chi = \chi' + i\chi''$. The fluctuation dissipation theorem yields[23]

$$\chi'' \propto \omega\langle|\delta\tilde{X}(\omega)|^2\rangle \tag{21}$$

relating the imaginary part of the susceptibility to the spectral density of the fluctuations in X.

3. Model Spectral Function

Application to compressional waves leads to the contribution of this "unifying model" of concentration fluctuations to the sonic attenuation per wavelength. It can be expressed by the spectral term

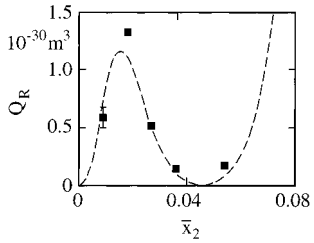

Figure 3. Romanov−Solov'ev amplitude parameter Q_R of aqueous solutions of tetra-*n*-propylammonium bromide at 25 °C displayed as a function of the equilibrium mole fraction $\bar{x}_2$ of salt. Figure symbols denote data derived from ultrasonic attenuation spectra.[7] The dashed curve represents the prediction from eq 23.

$$R_{um}(\nu) = Q\int_0^\infty \frac{q^2}{(1+0.164q\xi+0.25(q\xi)^2)^2}\frac{\omega\tau_g}{1+\omega^2\tau_g^2} \tag{22}$$

The amplitude parameter Q is assumed to be largely given by the Romanov−Solov'ev amplitude factor[15,16] Q_R which, according to the equation

$$Q_R = \frac{\rho c_s^2 kT_B}{8\pi}\frac{V^2}{g''^2}\left(\frac{v''}{V} - A\frac{h''}{c_p}\right) \tag{23}$$

is related to thermodynamic quantities. In eq 23 ρ is the density, k_B the Boltzmann constant, T the absolute temperature, V the molar volume, and A and c_p are the instantaneous thermal expansion coefficient and specific heat at constant pressure, respectively. The double-primed quantities

$$g'' = \partial^2 G_0/\partial^2 x_2, \quad v'' = \partial^2 V_0/\partial^2 x_2, \quad h'' = \partial^2 H_0/\partial^2 x_2 \tag{24}$$

are the second derivatives of the Gibbs free enthalpy, molar volume, and molar enthalpy, respectively. The subscript "0" is used to indicate that the values of the thermodynamic quantities have to be taken without contributions from fluctuation. Quantity $\bar{x}_2$ denotes the equilibrium mole fraction of the dispersed phase, the nonaqueous constituent in the mixtures under consideration. The calculation of second derivatives from experimental data is doubtless a difficult attempt. Nevertheless, for various liquid mixtures Q_R data derived from eq 23 have been found in reasonable agreement with experimental findings from ultrasonic attenuation spectrometry.[24−27] As an example, the Q_R-versus-$\bar{x}_2$ relation for aqueous tetra-*n*-propylammonium bromide solutions[7] is displayed in Figure 3 indicating that the predictions from the thermodynamic equations (eqs 23 and 24) fairly well fit to the relaxation measurements. Following Montrose and Litovitz[19] there may exist another contribution Q_S due to the relaxation with identical frequency behavior of the shear viscosity η_s. Assuming a linear superposition

$$Q = Q_R + Q_S \tag{25}$$

follows.

Since at $r \gg \xi$ the spatial correlations in fluctuations are assumed to follow the Ornstein−Zernike ansatz, the relation

$$\xi = k_B T/(6\pi\eta_s D) \tag{26}$$

by Kawasaki[13] and Ferrell[28] may be used to relate the characteristic correlation length ξ to the mutual diffusion coefficient. Equation 26 is identical with the Stokes−Einstein relation describing the diffusion of a spherical particle of radius ξ in a liquid with shear viscosity η_s. Utilizing eq 26 there are just three unknown parameters left in $R_{um}(\nu)$, namely Q, D, and

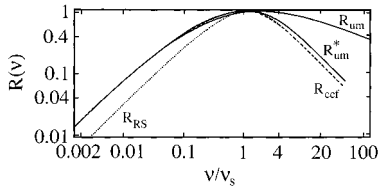

Figure 4. Shape of the relaxation spectral terms of the unifying model (R_{um}, $q_{max} \rightarrow \infty$) the modified version of this model (R^*_{um}, $q_{max} < \infty$) as well as of the original (R_{RS}) and the extended Romanov−Solov'ev (R_{ccf}) model. Parameter ν_s denotes the frequency of maximum excess attenuation ($d(\alpha\lambda)_{exc}/d\nu = 0$, $d^2(\alpha\lambda)_{exc}/d\nu^2 < 0$ at ν_s). Calculating R^*_{um}, q_{max} has been choosen so that $R^*_{um} \approx R_{ccf}$.

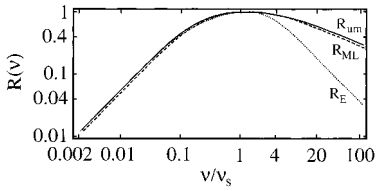

Figure 5. Shape of the relaxation spectral terms of the unifying model (R_{um}), the Montrose−Litovitz (R_{ML}), and the Endo (R_E) model. See Figure 4 for the meaning of ν_s.

τ_0. The latter quantity can be left out of consideration if no process with discrete relaxation time plays a significant role within the concentration fluctuation scheme. The values for the diffusion coefficient D derived from ultrasonic spectra may be compared to data that have been derived from other measurements, e.g., NMR studies. The amplitude parameter Q, in principle, can be verified by the thermodynamic measurements using eq 23.

The effect of a maximum wave vector $q_{max} < \infty$ in the spectral function is illustrated by Figure 4 where graphs of $R_{um}(\nu)$ are presented for both a finite q_{max} and also for $q_{max} \rightarrow \infty$. Because no analytical form exists for the integral in the spectral function (eq 22), the values of R_{um} have been calculated numerically using the Romberg method.[29] For this purpose a parameter q_M has been introduced up to which the calculation of the integral was performed. In order to verify that a sufficiently high q_M value had been chosen in the calculations, we always made sure that use of a larger q_M did not affect the spectral function within the frequency range under consideration. For the numerical calculations the substitutions

$$\tau_{q_M} = (Dq_M^2)^{-1}, \quad \vartheta = (q_M\xi)^{-1}, \quad \upsilon = \tau_{q_M}/\tau_0 \tag{27}$$

lead to the following form of eq 22

$$R_{um}(\nu) = \frac{Q\omega}{D\xi} \lim_{q_M \rightarrow \infty} \left[(q_M\xi)^{-3} \int_0^1 \frac{u^2}{(\vartheta^2 + 0.164\vartheta u + 0.25u^2)^2} \frac{u^2 + \upsilon}{(u^2 + \upsilon)^2 + (\omega\tau_{q_M})^2} du \right] \tag{28}$$

which has proven an adequate formulation also in the evaluation of measured spectra.

Also displayed in Figure 4 for comparison with $R_{um}(\nu)$ are the Romanov−Solov'ev function $R_{RS}(\nu)$[15,16] and the spectral function $R_{ccf}(\nu)$ representing the RS model as extended for the effect of spatial correlations of fluctuations.[7] To enable an easy comparison of their shape normalized spectral terms are shown in Figure 4. Due to the consideration of spatial correlations in the extended model, the $R_{ccf}(\nu)$ term in the low frequency range ($\nu < \nu_s$) obviously extends over a broader frequency band than the $R_{RS}(\nu)$ function. Because both spectra are based on an Ornstein−Zernike behavior of long range correlations, $R_{um}(\nu)$ and $R_{ccf}(\nu)$ display the same properties at $\nu < \nu_s$. Since no additional process with relaxation time τ_0 is taken into account here ($\tau_0 \rightarrow \infty$, $\tau_g = \tau_q$), the modified spectral function

$$R^*_{um}(\nu) = R_{um}(\nu, q_{max}, \tau_g = \tau_q) \tag{29}$$

of the unifying model also almost agrees with $R_{ccf}(\nu)$ at $\nu > \nu_s$ in accordance with our expectations. Integration over the complete q space ($q_{max} \rightarrow \infty$), however, results in significant changes in the high frequency part of the spectral function ($R_{um}(\nu) > R^*_{um}(\nu)$, $\nu > \nu_s$), indicating that high q components in the fluctuations add noticeable contributions to the high frequency part of the absorption spectrum. As Romanov and Solov'ev already pointed out in their pioneering paper,[15,16] spectral functions that are based on the assumption of a minimum interaction length l_m, therefore, apply only up to the frequency ν_s of the maximum $R(\nu)$ value.

In Figure 5 the model spectral functions $R_{um}(\nu)$, $R_{ML}(\nu)$, and $R_E(\nu)$ from the unifying model as well as the Montrose-Litovitz and the Endo theory, respectively, are presented. The three functions nicely agree at $\nu < \nu_s$. As a result of the assumption of an Ornstein−Zernike behavior also for small interactions, in conjunction with the assumption of a minimum interaction length l_m, in the Endo model, $R_E(\nu)$ exhibits significantly smaller values at $\nu > \nu_s$ than $R_{um}(\nu)$ and $R_{ML}(\nu)$. Figure 5 additionally indicates that the unifying model, up to high frequencies, provides an excellent approximation of the predictions by the Montrose−Litovitz theory.

4. Relaxation Time Distribution of the Fluctuation Model

Effects from the simultaneous action of the diffusive process and the reaction with relaxation time τ_0 may be additionally illustrated by the behavior of the relaxation time distribution function G_{um} corresponding with the spectral function R_{um}. Let τ^* denote a suitably chosen relaxation time, e.g., $\tau^* = 1$ ns here, and $r = ln(\tau/\tau^*)$. Then G_{um} is defined by

$$R_{um}(\nu) = Q \int_0^\infty G_{um}(r) \frac{\omega\tau}{1 + (\omega\tau)^2} dr \tag{30}$$

with

$$\int_0^\infty G_{um}(r) dr = 1 \tag{31}$$

For this unifying model G_{um} can be given in an analytical form

$$G_{um}(r) = 0 \qquad \text{at} \qquad \tau_0 < \tau < (D^2 q_M)^{-1} \tag{32}$$

and, using the substitution $q \rightarrow ((\tau^{-1} - \tau_0^{-1})/D)^{1/2}$

$$G_{um}(r) = G^*_{um} \frac{[e^r(1 - \tau^* e^r/\tau_0)]^{1/2}}{[e^r + 0.328(\tau_\xi e^r(1/\tau^* - e^r/\tau_0))^{1/2} + \tau_\xi(1/\tau^* - e^r/\tau_0)]^2} \tag{33}$$

otherwise. In eq 33 G^*_{um} is an amplitude following from relation 31 and

$$\tau_\xi = \xi^2/(4D) \tag{34}$$

is a characteristic relaxation time.

The relaxation time τ_0 of the stoichiometrically defined process constitutes the maximum time constant of the model. A prospective slower decay by diffusion of local fluctuations in concentration will be short circuited by the τ_0 mechanism. Relaxation times $\tau > \tau_0$, therefore, are missing in G_{um}. Parameter τ_ξ, as defined by eq 34, is another characteristic relaxation time of the model. It represents the decay time for which the integrand of eq 19 adopts its maximum value. Hence, to the corresponding component (with wave vector $(D\tau_\xi)^{-1/2}$ in the fluctuations) the strongest weight is given in the integral of the $R_{um}(\nu)$ function (eq 22). The characteristic time τ_ξ thus defines the location of G_{um} within the r space, whereas τ_0 determines the shape of the distribution function.

At some parameter values (τ_ξ, τ_0/τ_ξ) graphs of the relaxation time distribution function $G_{um}(r)$ are presented in Figure 6. In order to show the relative importance of the different molecular mechanisms on realistic conditions, parameter values as resulted from ultrasonic spectra for aqueous solutions of n-butylurea have been selected here.[9] For the 0.8 molar solution (τ_ξ, $\tau_0/\tau_\xi = 53$ ns, 5.3) a rather broad relaxation time distribution, as characteristic for diffusive processes, emerges. The cutoff by the τ_0 process around $r = 2.3$ plays only an insignificant role in the distribution function. Toward higher *n*-butylurea concentrations, the fluctuation correlation length ξ increases and the diffusion mechanisms slow down. Consequently, the characteristic relaxation time τ_ξ substantially shifts to higher values. As a result the decay of the concentration fluctuations is more and more governed by the stoichiometrically defined process with almost concentration independent τ_0, corresponding with a rather sharp cut off in $G_{um}(r)$ near $r = 3$ (Figure 6).

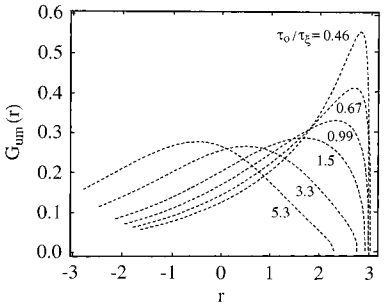

Figure 6. Relaxation time distribution function of the unifying model (eqs 32 and 33) at different characteristic relaxation times τ_ξ and relaxation time ratios τ_0/τ_ξ.

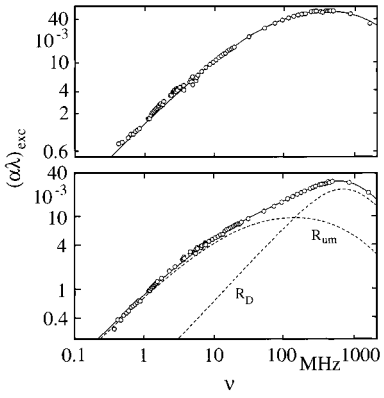

Figure 7. Ultrasonic excess attenuation spectrum of a 4.9 molar solution of *n*-propanol in water at 25 °C.[5] The full curve is the graph of the $R_{um}(\nu)$ spectral term with parameter values $Q = 20.7$ Å^3, $D = 1.3.10^{-10}$ m^2 s^{-1}, $\xi = 7.6$ Å, and $\tau_0 \rightarrow \infty$ (top). Spectrum of an 8.47 M aqueous solution of sec-butyl alcohol at 25 °C (bottom). Dashed curves show the subdivision of the spectrum into a R_{um} term ($Q = 8.2$ Å^3, $D = 0.67 \times 10^{-10}$ m^2 s^{-1}, $\xi = 10.1$ Å, $\tau \rightarrow \infty$) and a R_D term ($A_D = 0.046$, $\tau_D = 0.23$ ns).

5. Comparison with Ultrasonic Spectra of Binary Liquids

In order to verify the predictions of the unifying model we have fitted the $R_{um}(\nu)$ function to broadband ultrasonic spectra as measured for three series of binary liquids (i) aqueous solutions of urea and of its derivatives, (ii) monohydric alcohol/water mixtures, and (iii) mixtures of water with poly(ethylene glycol)monoalkyl ethers (C_iE_j). Depending on the hydrophobic/hydrophilic balance of the organic molecules, the tendency toward a microinhomogeneous structure of the aqueous systems is expected to vary significantly within each series. This is particular true for the monohydric alcohol/water and C_iE_j/water mixtures which include completely miscible systems and also such with miscibility gap.

Besides urea itself the first afore mentioned series includes methyl-, ethyl-, *n*-propyl-, and *n*-butylurea, as well as the isomers of the latter, tetramethyl-, *n*,*n*-diethyl-, and *n*,*n*′-diethylurea. The sonic parameters for the solutions of this series, with solute concentrations between 0.5 and 10.5 mol/L, are detailed discussed elsewhere.[9] We shall, therefore, focus on some general trends in the spectra here. Most interesting, the frequency dependent excess attenuation per wavelength for all solutions investigated within this first series can be well represented by the unifying model relaxation function $R_{um}(\nu)$. Only with the solutions of *n*-propylurea and *n*-butylurea a stoichiometrically defined process appears to be present. The experimental spectra of the other series (i) solutions can be well described analytically assuming $\tau_0 \rightarrow \infty$, thus applying the Romanov−Solov'ev model in its extended version $R_{ccf}(\nu)$ to account for spatial correlations of concentration fluctuations.

The spectra of both additional series of liquids can be also nicely described by the unifying model. Some mixtures call for an additional Debye term (eq 2). Also the ultrasonic spectra of some alcohols under investigation[5] follow a Debye type relaxation. For this reason, the spectral function

$$S_{tot}(\nu) = R_{um}(\nu) + R_D(\nu) + B\nu \tag{35}$$

has been used to represent the total absorption per wavelength spectra of the alcohol/water and the C_iE_j/water mixtures. Examples for experimental spectra and the corresponding model function $S_{tot}(\nu)$ without ($A_D \equiv 0$) and with ($A_D \neq 0$) Debye term $R_D(\nu)$ are shown in Figures 7 and 8, respectively.

It is worth noting that the ultrasonic spectra for all alcohol/water mixtures do not ask for a τ_0 process. Most spectra, therefore, besides the *B* parameter, which represents the limiting high frequency part in the attenuation coefficient, require just two adjustable parameters, *Q* and *D*. This is a remarkable result, since so far theoretical models of noncritical concentration fluctuations did not adequately apply for the experimental findings. For this reason the Fixman−Kawasaki model,[10−13] designed for critical systems, had been used to empirically represent the noncritical alcohol/water spectra.[5] As briefly mentioned above, spectra for some mixtures of high alcohol content exhibit additional Debye type relaxation behavior. A Debye term is also found for pure alcohols, it is suggested to be due to structural isomerization or association by hydrogen bonding of alcohol molecules.

Quite remarkably a reduced number of parameters is also required for the C_iE_j/H_2O mixtures. Only the C_4E_1/H_2O system

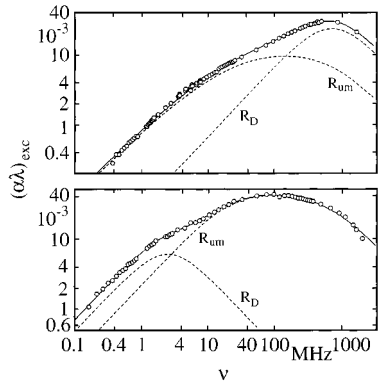

Figure 8. Ultrasonic excess attenuation spectrum of an 8.47 molar aqueous solution of *sec*-butyl alcohol (top[5]) and of a 2.6 M aqueous solution of 2-butoxyethanol (bottom[6]) 25 °C. Dashed curves show the subdivision of the spectra into a Debye term and a R_{um} term. The full curves represent the sum of both relaxation terms, respectively.

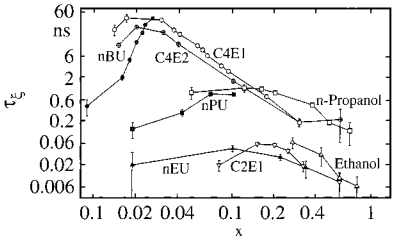

Figure 9. Characteristic relaxation time τ_ξ versus mole fraction x of the nonaqueous constituent for some aqueous systems at 25 °C. C2E1, 2-ethoxyethanol; C4E1, 2-butoxyethanol; C4E2, 2-(2-butoxyethoxy)-ethanol; nEU, *n*-ethylurea; nPU, *n*-propylurea; nBU, *n*-butylurea.

needs an additional Debye relaxation term $R_D(\nu)$ if the dominating part of the spectra is represented by the $R_{um}(\nu)$ function (Figure 8). The excess absorption spectra of the other liquids within the (iii) series can be well described by the unifying model. The C_2E_1/water mixtures, most of the i-C_3E_1/water mixtures, and even some of the C_4E_1/water mixtures, do not call for a τ_0 process. Hence again, in addition to the *B*-coefficient (eq 35), just parameters Q and D are necessary for an adequate description of various experimental spectra over the frequency range from 0.1 to 2000 MHz. These results may be taken to indicate that, in the spectral functions used so far for alcohol/water and C_iE_j/water mixtures under consideration, an additional Debye term was necessary to account for an incomplete consideration of noncritical concentration fluctuations rather than representing a specific molecular mechanism.

6. Hydrophobic Effects

The unifying model enables a common view of the results for the three series of liquids. Values of the parameters of the model are discussed in ref 9. Here we want to direct attention to some general trends in the behavior of the characteristic time τ_ξ reflecting the decay of concentration fluctuations by diffusion. The values of τ_ξ, according to eqs 26 and 34 following from the diffusion coefficient D and shear viscosity η_s data of the liquids,

$$\tau_\xi = \left(\frac{k_B T}{12\eta_s}\right)^2 \frac{1}{D^3} \tag{36}$$

within each series of mixture vary in a characteristic manner. For the constituents with unbranched alkyl group this effect is illustrated in Figure 9. This plot of τ_ξ data clearly points at three groups of liquids, differing in the number of carbon atoms per

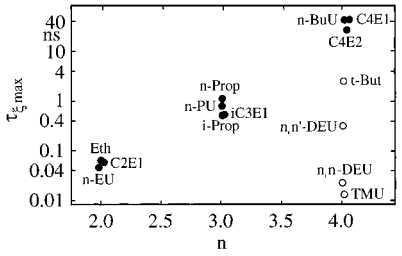

Figure 10. Maximum characteristic relaxation times $\tau_{\xi max}$ for some series of mixtures of water with organic constituents plotted against the number n of carbon atoms per alkyl group of the organic molecules. The following shorthand notations are used: Eth, ethanol; *n*-Prop, *n*-propanol; i-Prop, *iso*-propanol; t-Bu, *tert*-butanol; C2E1, 2-butoxyethanol; iC3E1, *iso*-propoxyethanol; C4E2, 2-(2-butoxyethoxy)ethanol; n-EU, *n*-ethylurea; n-PU, *n*-propylurea; n-Bu, *n*-butylurea, *n,n*-DEU, *n,n′*-diethylurea; n,n-DEU, *n,n*-diethylurea; TMU, tetramethylurea.

alkyl group of the nonaqueous constituent. This result also indicates the minor role which the hydrophilic groups of the organic molecules play in the dynamics of concentration fluctuations.

As expected intuitively there exists a relative maximum in the τ_ξ values as a function of mole fraction x. With increasing alkyl group length the composition x_{max} at which this maximum occurs shifts to smaller mole fraction of the organic constituent. For a clear view of the concentration fluctuation characteristics of all liquids under study, in Figure 10 a plot of the maximum decay time $\tau_{\xi max} = \tau_\xi(x_{max})$ for each binary system is given as a function of the number n of carbon atoms per alkyl group. This diagram confirms the uniform concentration fluctuation properties of molecules with unbranched alkyl groups, exhibiting a strong increase in $\tau_{\xi max}$ when going from $n = 2$ to $n = 4$. It also clearly shows a substantial effect of branching of the alkyl groups, particularly for the isomers of *n*-butylurea. The maximum τ_ξ value resulting for the *n,n′*-diethylurea solutions is smaller than $\tau_{\xi max}$ for n-butylurea by the remarkable factor of 100. For solutions of *n,n*-diethylurea and especially of tetramethylurea $\tau_{\xi max}$ is even reduced by another factor of 20, adopting values around 10 ps which is in the order of the molecular reorientation times.[30]

The τ_ξ data derived from the ultrasonic spectra of aqueous solutions strongly support the idea of concentration fluctuations to be substantially promoted by alkyl groups of the nonaqueous constituent. Effects of isomerization and thus of the steric arrangement of the hydrophobic groups are also most important for the formation of a microinhomogeneous liquid structure. As unbranched alkyl groups are most effective in promoting long-ranging correlations in fluctuations we suggest that "premicellar" hydrophobic interactions between these groups are the dominant factor in the molecular dynamics of microheterogenity.

References and Notes

(1) Bhattacharjee, J. K.; Ferrell, R. A. *Phys. A* **1998**, *250*, 83.
(2) Mirzaev, S. Z.; Telgmann, T.; Kaatze, U. *Phys. Rev. E.* **1999**. In press.
(3) Schreiber, U. Dissertation, Georg-August-Universität, Göttingen, 1988.
(4) Menzel, K. Dissertation, Georg-August-Universität, Göttingen, 1993.
(5) Brai, M.; Kaatze, U. *J. Phys. Chem.* **1992**, *96*, 8946.
(6) Menzel, K.; Rupprecht, A.; Kaatze, U. *J. Phys. Chem. B* **1997**, *101*, 1255.
(7) Kühnel, V.; Kaatze, U. *J. Phys. Chem.* **1996**, *100*, 19747.
(8) Rupprecht, A.; Kaatze, U. *J. Phys. Chem. A* **1997**, *101*, 9884.
(9) Rupprecht, A. Dissertation, Georg-August-Universität, Göttingen, 1997.
(10) Fixman, M. *J. Chem. Phys.* **1960**, *33*, 1364.

(11) Fixman, M. *Adv. Chem. Phys.* **1964**, *4*, 175.
(12) Kawasaki, K. *Phys. Rev. A* **1970**, *1*, 1750.
(13) Kawasaki, K. *Ann. Phys. (N.Y.)* **1970**, *61*, 1.
(14) Debye, P. *Polare Molekeln*; Hirzel: Leipzig, 1929.
(15) Romanov, V. P.; Solov'ev, V. A. *Sov. Phys. Acoust.* **1965**, *11*, 68.
(16) Romanov, V. P.; Solov'ev, V. A. *Sov. Phys. Acoust.* **1965**, *11*, 219.
(17) Romanov, V. P.; Solov'ev, V. A. In *Water in Biological Systems*; Vuks, M. F., Sidrova, A. J., Eds.; Consultant Bureaus: New York, 1971; Vol. 2, p 1.
(18) Romanov, V. P.; Ul'yanov, S. V. *Phys. A* **1993**, *201*, 527.
(19) Montrose, C. J.; Litovitz, T. A. *J. Acoust. Soc. Am.* **1970**, *47*, 1250.
(20) Endo, H. *J. Chem. Phys.* **1990**, *92*, 1986.
(21) Ornstein, L. S.; Zernike, F. *Phys. Z.* **1918**, *19*, 134.
(22) Orstein, L. S.; Zernike, F. *Phys. Z* **1926**, *27*, 762.
(23) Kohler, F. *The Liquid State*; Verlag Chemie: Weinheim, 1972.
(24) Blandamer, M. J.; Waddington, D. *Adv. Mol. Relax. Processes* **1970**, *2*, 1.
(25) Davenport, J. M.; Dill, J. F.; Solov'ev, V. A.; Fritsch, K. *Sov. Phys. Acoust.* **1968**, *14*, 236.
(26) Atkinson, G.; Rajagopalan, S.; Atkinson, B. L. *J. Chem. Phys.* **1980**, *72*, 3511.
(27) D'Arrigo, G.; Paparelli, A. *J. Chem. Phys.* **1988**, *88*, 7687.
(28) Ferrell, R. A. *Phys. Rev. Lett.* **1970** *24*, 1969.
(29) Hämmerlin, G.; Hoffmann, K.-H. *Numerische Mathematik*; Springer: Berlin, 1994.
(30) Kaatze, U.; Gerke, H.; Pottel, R. *J. Phys. Chem.* **1986**, *90*, 5464.